

Monitoring of thermo-hydrological behaviour in Green Infrastructure

Anil Yildiz^{1,2}, Ross A. Stirling^{1,2}, and Stephanie Glendinning²

¹National Green Infrastructure Facility, Newcastle upon Tyne, NE4 5TG, United Kingdom

²School of Engineering, Newcastle University, Newcastle upon Tyne, NE1 7RU, United Kingdom

Abstract. The multi-purpose nature of Sustainable Drainage Systems (SuDS) or Green Infrastructure (GI) presents a significant opportunity to store or recover heat for low carbon urban heating/cooling systems. The capacity of such systems for energy storage is strongly dependent on the thermal and hydrological boundary conditions, estimation of their feasibility requires a deep understanding of how atmospheric conditions and the near-surface hydrological regime affect heat transfer. A large-scale, outdoor lysimeter has been set up at the (UK) National Green Infrastructure Facility in order to monitor the influence of atmospheric conditions on hydrological and thermal properties of SuDS. Volumetric water content, matric suction and temperature were monitored at various depths and locations within the sand and topsoil layer. Additionally, thermal conductivity at multiple depths, and heat flux at the surface and bottom boundary were measured. Results of the initial monitoring phase, as well as, preliminary laboratory tests are presented herein and demonstrate the complex interaction between partial saturation and heat transfer. Further work investigates the effects of rainfall and heat injection using rainfall simulation and a variable-power heating cable, respectively.

1 Introduction

Exploitation of the ground as a sustainable heat resource continues to gain momentum due to increasing energy demand, environmental impact reduction and urban resilience to climate change and increased population density. A notable part of the overall energy consumption is due to space heating and cooling [1]. Ground heat exchangers (GHE) are long-term, durable and highly efficient alternatives to conventional building heating and cooling systems [2].

A novel way to increase efficiency, reduce initial capital cost and reduce valuable land uptake to provide affordable GHE systems is to utilise existing or to-be-built green infrastructure. Sustainable Drainage Systems (SuDS), are multi-beneficial, durable and sustainable alternative to conventional, buried infrastructure solutions to urban flood problems.

The efficiency of GHE is strongly governed by the thermal conductivity of the medium in which they are installed. The thermal conductivity of soils is determined by the volumetric proportion of soil, water and air phases. An investigation into the feasibility of utilising SuDS for heat source/sinks requires an understanding of their thermal and hydrological behaviour and boundary conditions. First attempts to test varying components of SuDS in combination with GHE have been made on pervious paving systems [3] and swales [4].

The work presented here investigates the potential use of a pilot-scale SuDS as a heat exchange site via a heavily-instrumented, vegetated lysimeter setup exposed to naturally occurring atmospheric conditions. The objectives are to monitor the hydrological changes in the

soil and the response of soil to these changes in terms of thermal properties.

2 Materials & methods

2.1 Outdoor laboratory & lysimeters

The National Green Infrastructure Facility (NGIF) is located in Newcastle-upon-Tyne in the northeast of the UK. NGIF is a living laboratory for innovative research into green infrastructure approaches via at-scale functional, heavily monitored SuDS. In addition to hydro-geotechnical laboratory facilities, the external experimental features comprise an array of lysimeters, in-ground bioretention cells and an extreme event swale which are all coupled with advanced sensing networks.

The lysimeter setup used in this research, shown in Fig. 1, comprises a stainless-steel cylindrical vessel 1200 mm in height with a diameter of 2000 mm and a conical bottom in order to collect and drain the water that infiltrates through the soil column. It is equipped with a flow gauge to measure the amount of water draining from the soil. A comprehensive weather station situated directly above the lysimeter measures air temperature, relative humidity, wind speed and direction, rainfall, and net radiation. An adjacent enclosure houses the dataloggers and a computer to record and upload data in real-time to dedicated NGIF servers. All data presented in this work can be accessed via an open access API (See <https://api.ngif.urbanobservatory.ac.uk/>).

* Corresponding author: anil.yildiz@newcastle.ac.uk



Fig. 1. Lysimeter setup at the National Green Infrastructure Facility after germination.

2.2 Soil

A fine sand was used in this study, which was classified as a poorly graded sand (SP) according to Unified Soil Classification (USCS). Index properties of the sand used in the lysimeter are given in Table 1.

Saturated hydraulic conductivity was determined according to the falling head technique on a sample prepared at a dry density of 1.43 Mg/m^3 in a 250 ml ring using KSAT[®] [5]. Saturated hydraulic conductivity was found to be $1.73 \times 10^{-4} \text{ m/s}$ as the mean value of three measurements. Further tests on samples prepared at minimum and maximum dry density (See Table 1) yielded mean saturated hydraulic conductivity values of 2.05×10^{-4} and $9.10 \times 10^{-5} \text{ m/s}$, respectively.

Table 1. Index properties of the sand.

Gravel – Sand – Fines	[%]	0 – 99 - 1
D₁₀ – D₃₀ – D₆₀	[mm]	0.10 - 0.17 - 0.24
C_u – C_c	[-]	2.4-1.2
Min. – max. dry density	[Mg/m³]	1.36-1.64

The Soil Water Retention Curve (SWRC) was obtained using a HYPROP[®] [3] setup and the same sample subsequent to the hydraulic conductivity tests. Measured gravimetric water content data was converted into volumetric water content, and van Genuchten equation was fitted to the calculated volumetric water content – measured matric suction data, given in Fig. 2, with a Levenberg-Marquardt non-linear least square algorithm using the R package “minpack.lm”. Fitting parameters are also given in Fig. 2.

Topsoil used in this study is a high fertility and organic rich substrate, certified to BS3882:2015 standards. It contains 79 % sand, 13 % silt and 8 % clay.

Organic matter, determined by loss-on-ignition, was 3.4 %, and carbon:nitrogen ratio was 12:1 [6].

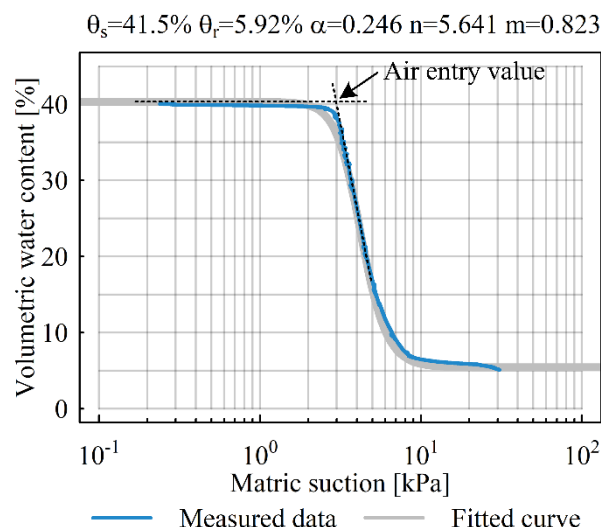


Fig. 2. Soil water retention curve of the sand used in the study.

2.3 Test setup

The bottom of the lysimeter was filled with gravel (nominally 20 mm) to provide free drainage until a clear height of 1000 mm was obtained. Gravel layer was topped with a nonwoven geotextile to filter the fine particles and to prevent clogging. A double-walled HDPE pipe, acting as a thermal insulator, with an inner diameter of 1800 mm and a wall thickness of 80 mm was placed concentric in the lysimeter to build the soil column. It consists of an 800 mm high sand layer, covered with 150 mm of topsoil.

Sand at its in-situ gravimetric water content (6-7 %) was mixed to obtain a target gravimetric water content of 16 %. A target relative density of 35% resulted in a dry density of 1.45 Mg/m^3 and a bulk density of 1.68 Mg/m^3 . Compaction was performed at every 100 mm by using a hammer with a weight of 6 kg, until the desired height in the pipe was reached. Core-cutter density measurements were taken after compaction at each layer, which provided a mean bulk density of 1.67 Mg/m^3 at an average gravimetric water content of 16.6%.

Topsoil was placed directly above the sand column, and no compaction was applied so as not to hinder plant growth. The total mass of the 150 mm thick topsoil layer was 460 kg, which gives an overall bulk density of 1.20 Mg/m^3 . Topsoil was sown with winter grazing ryegrass seeds (*Secale cereale*).

In order to later simulate heat injection, two heating cables were placed 100 mm above the bottom of the sand layer, each with a length of 10 m and a power input of 10 W/m at 220 V. Data presented herein covers the period before the heat injection tests.

2.4 Instrumentation

Measurement of hydrological parameters

Volumetric water content and matric suction were measured with Decagon 5TE and MPS6 sensors, respectively. Each sensor provides soil temperature data, as well. Two sensors of each were placed 200 mm from the centre in the topsoil layer at 150 mm depth, and in the sand layer at 250, 350, 450, 550, 650 and 750 mm below the topsoil surface. Data were recorded at 1 min intervals.

Measurement of thermal parameters

Heat flux at the surface and at the bottom of the sand layer were measured with two Hukseflux HFP01 heat flux plates. Thermal conductivity of the sand was measured with Hukseflux TP01 sensors at 250, 350, 550 and 750 mm. Hukseflux STP01 temperature profiler was inserted at the centre providing soil temperature measurements at 70, 100, 150, 250 and 550 mm. Additional soil temperature sensors, Campbell 107, were placed in the close vicinity of the heating cable. Data from these sensors were recorded at 30 sec intervals.

3 Rainfall data

All the data presented herein covers a period of 37 days from 01.06.2019 to 08.07.2019. Fig. 3 shows the daily total rainfall, defined as the summation of precipitation from 00:00 to 23:59, during the period of investigation. Total precipitation was 150.2 mm. Maximum daily total rainfall was recorded as 45.8 mm.

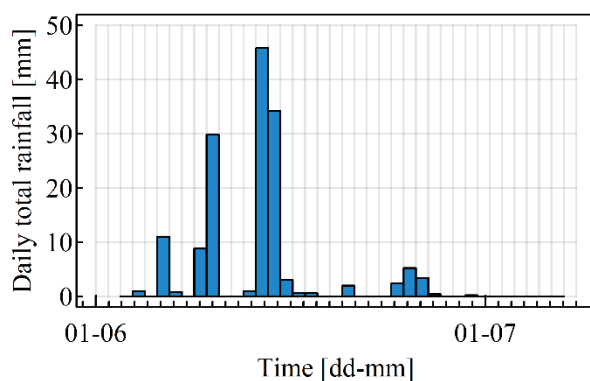


Fig. 3. Daily total rainfall during the period of investigation.

Two major rainfall events, responsible for 109.8 mm of the total rainfall and shown as textured bars in Fig. 3, provided 73.1% of the rainfall during the monitoring period and approximately 16% of the mean annual rainfall in 3 days [5].

The first event took place between 08.06.2019 and 09.06.2019, and a total rainfall of 29.8 mm was recorded. The second major event consisted of discontinuous rainfall between 12.06.2019 and

14.06.2019, total precipitation during this event was 80.0 mm.

One of the main functions of green infrastructure is to provide permeable areas with high infiltration and water retention capacity in typically impermeable urban settings. Total precipitation from these two major events can be translated into a volume of water of 75.8 and 203.7 litres, respectively, considering the surface area of the soil column as the catchment area. Total volume of rainfall during the period of investigation was 382.4 L, of which 188.9 L drained from the bottom of the soil column.

4 Hydrological parameters

4.1 Volumetric water content

Data from each sensor at every depth were divided into 30 min windows and averaged over this period. Then, the mean value from both sensors at each depth were calculated. Fig. 4 shows how the volumetric water

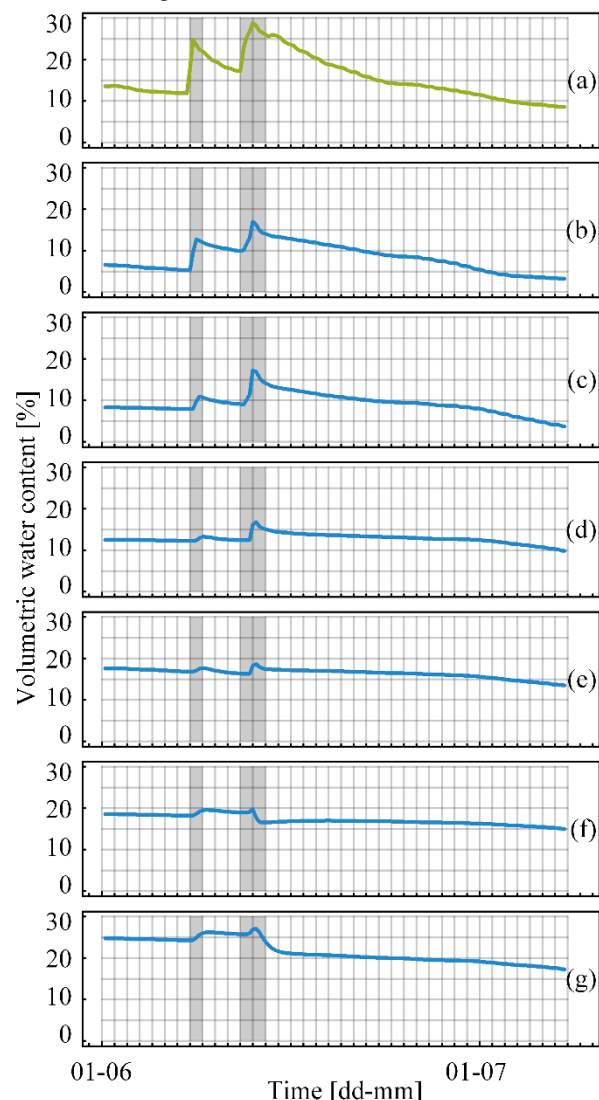


Fig. 4. Volumetric water content profiles during the period of investigation in the topsoil at (a) 100 mm, in the sand at (b) 250, (c) 350, (d) 450, (e) 550, (f) 650, (g) 750 mm. Grey marked areas show the major rainfall events.

content data varies with depth and in time in the soil column. It should be noted that Fig. 4a presents measurements from topsoil, whereas the Fig. 4b-4g are from the sand.

Similar trends were observed at every depth regardless of soil type. There is a substantial difference in terms of magnitude of volumetric water content in topsoil at 100 mm and in sand at 250 mm depth throughout the period of monitoring, which is due to differences in hydraulic conductivity and water retention characteristics of the two soil types used in this study.

4.2 Matric suction

Suction sensors used in this study, MPS-6 from Decagon Devices, Inc, start recording values from 9 kPa and the accuracy is 10% of the reading with an additional 2 kPa [6], any value around 10-15 kPa would mean suction can be less than the actual reading. As the air entry value of the sand used in this study is 3 kPa (See Fig. 2), it is hard to comment on the saturation of the sand column because it is not in the measurable range of the suction sensor.

Only the sensors in the topsoil and in the shallowest layer of the sand column recorded suction values during this period. Layers below 350 mm depth did not have measurable matric suction values using widely available dielectric permittivity-based suction monitoring technology.

Fig. 5 illustrates the suction generation in topsoil, at 100 mm depth, and in sand, at 250 mm depth. As the soil types are different, their responses to changes in the volumetric water content are also different. Measurements at 250 mm show that there were no significant changes in suction in the sand layer due to the major rainfall events in June 2019. Suction values rise to 20 kPa for the first time starting from 01.07.2019 and continued to increase to 523 kPa at the end of the period of investigation.

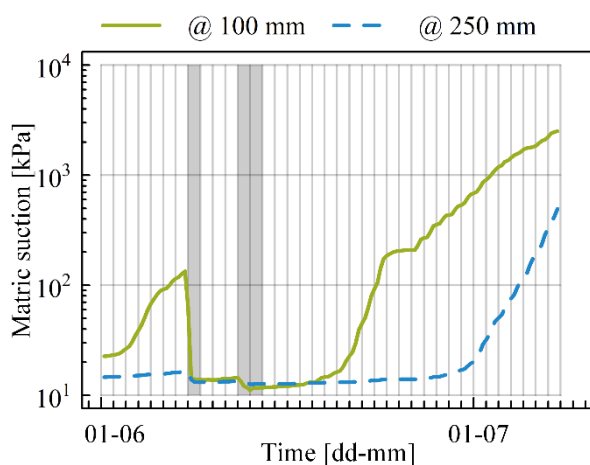


Fig. 5. Suction generation in topsoil at 100 mm, and in sand at 250 mm depth. Grey marked areas show the major rainfall events.

The topsoil layer shows an initial matric suction of 22 kPa at the beginning of the monitoring phase

presented herein, which increased to 138 kPa prior to the first major rainfall event. The generated suction was lost subsequent to the rainfall, and values dropped to the unmeasurable range, i.e. between 9 to 15 kPa, and stayed in this range until shortly following the second event. Suction is then seen to increase, except during a period of 2 days, before continuing to increase to 2560 kPa at the end of the monitoring window.

4.3. Completing the SWRC with field data

The field derived SWRC for the sand has been plotted using the volumetric water content and matric suction data from the sensors at 250 mm depth from the surface between 01.07.2019 and 08.07.2019, in which a significant amount of suction was generated, and can be considered as the first major drying event.

Due to the aforementioned inability of measuring low suction values with the dielectric permittivity sensors, the initial part of the SWRC could not be captured in the field. However, laboratory SWRCs were determined using tensiometers. Typically, tensiometer installations in the field are labour intensive in terms of maintenance, i.e. cavitation and refilling, and potentially introduce preferential vertical flow paths. Therefore, the field SWRC and laboratory SWRC of sand have been superimposed in Fig.6. It can be seen that field and laboratory data are in agreement, and form a complete SWRC profile for a wide matric suction range.

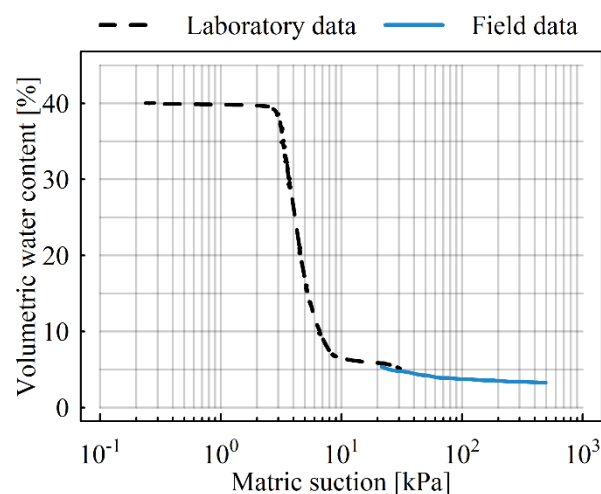


Fig. 6. Complete soil water retention curve of the sand.

4.4. Response to rainfall

Four volumetric water content values were chosen to compare the response to rainfall of topsoil and sand at different depths. Fig. 7 shows the water content values at the start of the monitoring campaign, the maximum values during the first and second rainfall event, and at the end of the monitoring campaign.

Event 1 caused a significant increase in water content up to a depth of 350 mm, a minor increase at 450 mm and did not infiltrate below that depth. Highest increase in water content was at 100 mm in the topsoil. As Event 2 was a prolonged rainfall event, water content increased

at all depths, and the magnitude of the increase reduced with depth. Drying after Event 2 resulted in water content values less than those at the beginning of the monitoring campaign.

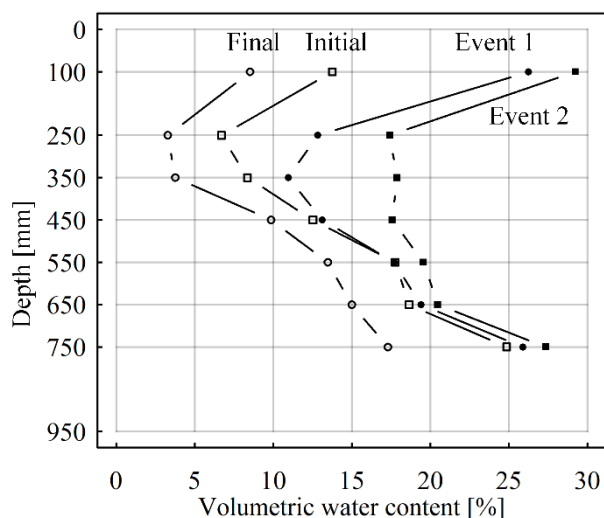


Fig. 7. Variation of water content with depth in the beginning and at the end of the monitoring period, as well as during major rainfall events.

5 Thermal parameters

5.1 Soil temperature

Fig. 8 provides the soil temperature, both in the topsoil and sand, and how it changes with depth and in time, as well as the air temperature. Data presented is based on 6-hourly means.

Maximum soil temperature during the period of investigation was 19.7 °C, and it was measured at 70 mm

below the surface, whereas the minimum value was 9.4°, which was measured 40 mm below the surface. Mean temperature in the sand throughout monitoring did not change significantly with depth. i.e. ranging between 13.9 °C – 14.2 °C.

Mean air temperature of the same period was 13.9 °C. The functionality of ground heat exchangers is also based on the similarities between the soil temperature at deeper layers and mean annual temperature [7]. Although the height of the soil column in the lysimeter is less than the depths at which conventional ground heat exchangers are typically installed, the mean air temperature and soil temperature was nearly identical for the duration of the monitoring presented herein.

Diurnal changes in air temperature are reflected as the change in soil temperature up to a depth of 150 mm, which is the interface between the topsoil and sand. Soil temperature is affected much less by the changes in the daily cycle of air temperature below 250 mm depth.

The significant increase in the air temperature starting shortly before July 2019 causes a simultaneous increase at shallow depth (e.g. less than 100 mm) in the topsoil, but the propagation of the increased temperature lags with depth in the sand.

5.2 Thermal conductivity

Thermal conductivity is a key parameter for the analysis of heat transfer in soil and is crucial in design calculations for ground heat exchangers. It is dependent on soil texture, mineral composition, water content, and bulk density [8]. It increases with increasing density and water content [9].

Fig. 9 shows the variation of thermal conductivity of sand measured at 250 mm depth. Volumetric water content at the same depth has also been plotted in the same figure to provide comparison. The minimum and

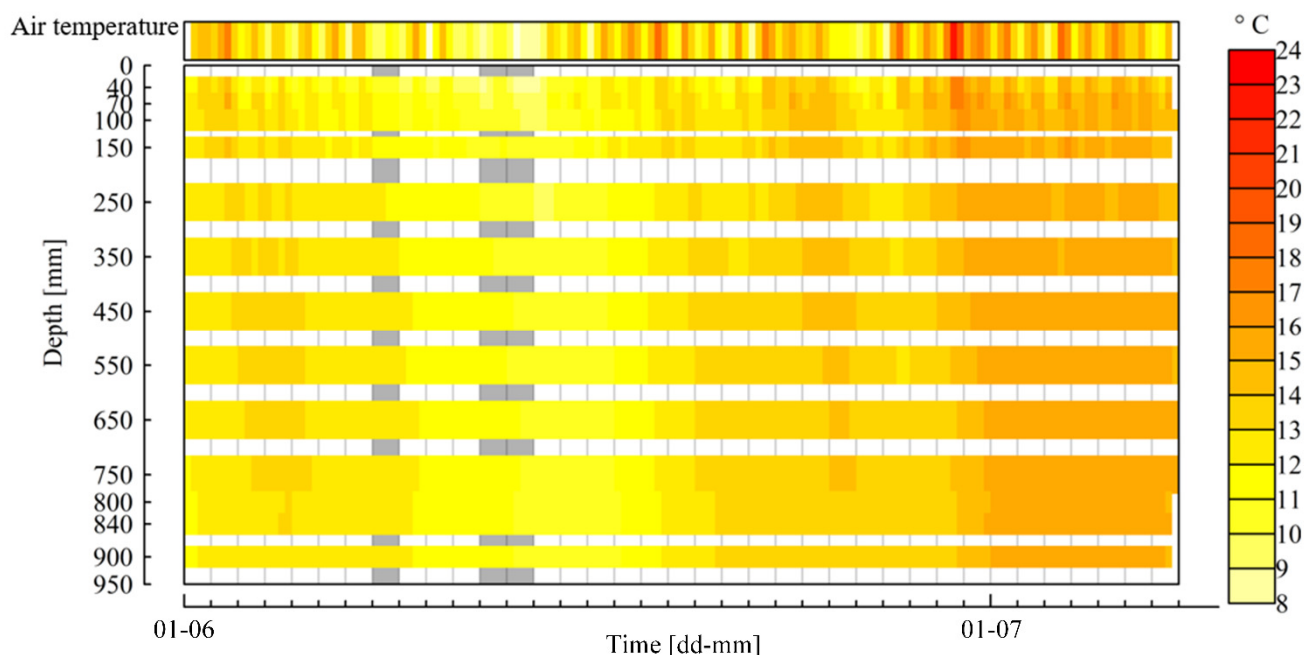


Fig. 8. Variation of soil temperature, recorded by different sensors, with depth and in time. Two major rainfall events are marked with grey rectangular background.

maximum thermal conductivity measured at 250 mm depth were 0.65 and 1.46 W/mK, respectively.

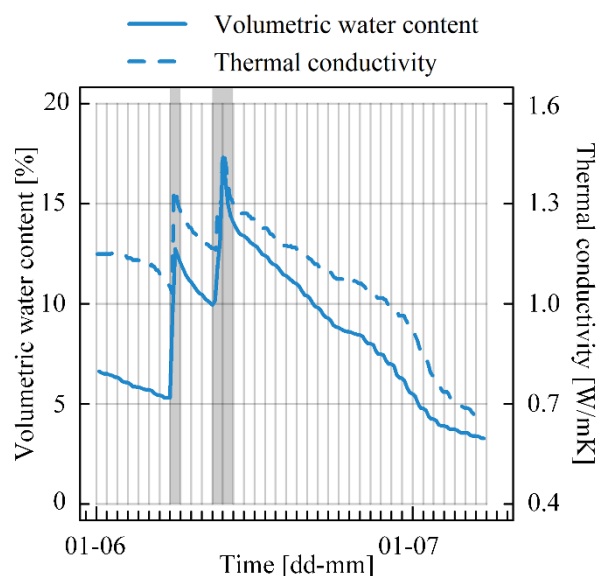


Fig. 9. Thermal conductivity and volumetric water content measured at 250 mm.

A sudden increase in thermal conductivity can be noted in the figure at the same point of the increase in water content which was due to the major rainfall events. A maximum value was reached at the end of Event 2, and thermal conductivity decreased constantly from that point. An agreement between the trend of the volumetric water content and thermal conductivity is clearly visible in Fig. 9.

A comparison of thermal conductivity at the same magnitude of water content before rainfall and due to drying after rainfall yields different values, which might suggest a hysteretic behaviour in thermal conductivity related to a change in grain packing.

6 Conclusions

The results from the monitoring campaign of the lysimeter setup is presented in this study. Changes in volumetric water content due to rainfall, and subsequent effects of these changes on the matric suction and thermal conductivity are discussed. Future research will focus on heat dissipation from a simulated building cooling system and testing under extreme rainfall events with an artificial rainfall simulator.

Acknowledgments

This study was funded by the EPSRC grant PLEXUS - Priming Laboratory EXperiments on infrastructure and Urban Systems (EP/R013535/1) and hosted by the UKCRIC National Green Infrastructure Facility (EP/R010102/1). The authors are thankful to technicians Gareth Wear, Michael Finley and Kevin Stott for the help during the setup of the experiment.

References

1. A.A. DiCarlo, R.A. Caldwell, SME 2018 12th Int. Conf. on Energy Sustainability (2018)
2. S.K. Soni, M. Pandey, V.N. Bartaria, *Renew. Sust. Energ. Rev.*, **47** 83-92 (2015)
3. S.M. Charlesworth, A.S. Faraj-Llyod, S.J. Coupe, *Renew. Sust. Energ. Rev.*, **68** 912-919 (2017)
4. C. Rey-Mahía, L.A. Sañudo-Fontaneda, V.C. Andrés-Valeri, F.P. Álvarez-Rabanal, S.J. Coupe, J. Rocas-García, *Sustainability* **11** 3118 (2019)
5. <https://www.metergroup.com/environment/products/>
6. <https://www.green-tech.co.uk/specialist-top-soils/top-soil/green-tree-topsoil>
7. SAAR 1961-1990 (1993)
8. http://manuals.decagon.com/Retired%20and%20Discontinued/Manuals/13755_MPS-2and6_Web.pdf
9. D. Banks, *An Introduction to Thermogeology: Ground Source Heating and Cooling* (John Wiley and Sons, 2012)
10. D.A. DeVries *Physics of Plant Environment* (1963)
11. N. Abu-Hamdeh, R. Reeder *Soil Science Society of America Journal* **64** 1285-1290 (2000)